MIT Libraries | DSpace@MIT

MIT Open Access Articles

Analysis of rapid C[sub n][sup 2] fluctuations observed during a 5-km communication link experiment

The MIT Faculty has made this article openly available. ***Please share*** how this access benefits you. Your story matters.

Citation: Yarnall, Timothy M. et al. "Analysis of rapid C[sub n][sup 2] fluctuations observed during a 5-km communication link experiment." Atmospheric Propagation VI. Ed. Linda M. Wasiczko Thomas & G. Charmaine Gilbreath. Orlando, FL, USA: SPIE, 2009. 73240B-7. © 2009 SPIE

As Published: http://dx.doi.org/10.1117/12.818795

Publisher: Society of Photo-optical Instrumentation Engineers

Persistent URL: http://hdl.handle.net/1721.1/52702

Version: Final published version: final published article, as it appeared in a journal, conference proceedings, or other formally published context

Terms of Use: Article is made available in accordance with the publisher's policy and may be subject to US copyright law. Please refer to the publisher's site for terms of use.

Massachusetts Institute of Technology

Analysis of rapid C_n^2 fluctuations observed during a 5 km communication link experiment

Timothy M. Yarnall, Steven S. Michael, John D. Moores,
Ronald R. Parenti, William E. Wilcox Jr.

Massachusetts Institute of Technology Lincoln Laboratory,
244 Wood Street, Lexington MA, USA

ABSTRACT

The path-integrated turbulence strength is usually thought of as a parameter that varies slowly with time. In a recent free-space communications experiment the C_n^2 value over a 5-km horizontal path was monitored almost continuously for a period of nearly a month. In addition to well defined and repeatable diurnal fluctuations, strong short-term fluctuations were observed in which the turbulence strength changed by an order of magnitude within a period of minutes. These rapid changes were independently measured by a commercial scintillometer and the high-rate output from the communications transceiver. The characteristics and probable causes for these dynamic atmospheric events and their impact on the design of free-space communication systems are discussed in this article.

Keywords: Scintillation, atmospheric propagation, optical communications, gamma-gamma distribution

1. INTRODUCTION

When compared to radio-frequency systems, atmospheric optical communications links offer several advantages such as small power requirements, high data rates, and low probability of interception; however, the atmospheric channel, through turbulence induced scintillation, poses a singular challenge to performing error-free communications.[1] Modern high-speed communications receivers typically utilize single-mode fiber and require the input power in fiber P_f to exceed a minimum level, the sensitivity, for error-free operation. Fading events can occur quite frequently and be severe enough to cause P_f to fall below the receiver sensitivity and create errors. There are many techniques for combating scintillation: spatial diversity,[2–5] using multiple transmit or receive apertures; temporal diversity,[6,7] interleaving the data to add resilience to outages; and channel coding[6,8,9] to name a few. For proper implementation these techniques all require knowledge of the distribution of P_f which in turn depends on the statistical properties of the atmosphere foremost of which is C_n^2 the turbulence strength. Many approaches to predicting the distribution of P_f from C_n^2 have been presented in the literature.[10–12] There are also models for determining C_n^2 from local environmental conditions[12] and link geometry.[11] In this paper, we discuss a communications experiment in which P_f and C_n^2 were both monitored with particular attention paid to fluctuations in C_n^2 and the impact of those fluctuations on the distribution of P_f and overall communications performance.

2. EXPERIMENT

A 1550-nm lasercom system employing a single transmitter and a spatial-diversity receiver operated over a period of three months in the late summer and fall of 2008. The link spanned a 5.4 km horizontal path over forested hills and connected a fire observation tower in Groton, MA to the Firepond observatory dome in Westford, MA as shown in Fig. 1. The single transmitter and four receiver apertures, all stationary, were 12 mm in diameter. Five identical and independent tracking systems (one for each fiber) provided gross tilt correction. Measurements of the optical power P_f coupled into each of the single mode fibers were recorded at a 1-kHz rate by New Focus 2103 HighDynamic-range (75 dB) log power meters. The tracking systems were not stressed by the channel and operated for more than 24 hours without losing lock and did not introduce appreciable

Correspondence to TMY: timmy@LL.mit.edu

Atmospheric Propagation VI, edited by Linda M. Wasiczko Thomas, G. Charmaine Gilbreath,
Proc. of SPIE Vol. 7324, 73240B · © 2009 SPIE · CCC code: 0277-786X/09/$18 · doi: 10.1117/12.818795

Downloaded from SPIE Digital Library on 15 Mar 2010 to 18.51.1.125. Terms of Use: http://spiedl.org/terms

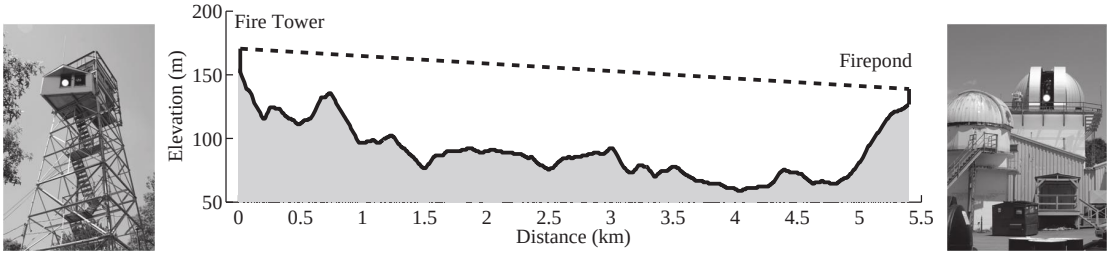

Figure 1. From left to right: transmitter at the fire observation tower, height profile of the link, and receiver at the Firepond observatory.

fluctuation in P_f. Independent channel characterizations were made by a Scintec BLS900 scintillometer. The Scintec instrument measured σ_I^2 and estimated the path-integrated turbulence strength C_n^2 every two minutes and ran nearly continuously throughout the experiment. Meteorological conditions (temperature, barometric pressure, wind speed, wind direction, solar radiation, *etc.*) were monitored by a weather station and recorded once per minute. Although the primary motivation for the experiment was the demonstration of the lasercom link, a great deal of environmental data was recorded with an aim to aid in the design of future links and to confirm the predictions of channel models for scintillation. This paper focuses in the scintillation properties of this channel.

3. RESULTS

The Scintec scintillometer was operated nearly continuously for two months; however, at times inclement weather, usually rain, precluded any measurements from being made. In Fig. 2 a scatter plot of C_n^2 vs time of day clearly shows the diurnal variations in C_n^2. The morning and afternoon quiescent periods are both discernable as are the daytime and nighttime spans where C_n^2 is relatively stable. The morning transition is not as sharply defined as the afternoon transition; this may be attributable to frequent presence of morning fog. It was observed that the daytime C_n^2 was largely confined to a band from 8×10^{-16} to 10^{-14} $\mathrm{m}^{-2/3}$ while the nighttime values range from 8×10^{-18} to 2×10^{-14} $\mathrm{m}^{-2/3}$ and was often found to be higher than the preceding daytime values. There were, however, times other than the quiescent periods, when the C_n^2 varied by an order of magnitude over a period of minutes. These rapid fluctuations were strongly correlated with P_f measurements and were caused at least in part by changes in the cloud cover.

Meteorological conditions were monitored by a Davis Instruments Vantage Pro2 weather station. In Fig. 3 the simultaneously recorded values for C_n^2 and the incident solar radiation are displayed for three consecutive days. The first day, starting at midnight, begins with a fairly constant C_n^2 until sunrise and was immediately followed by a dip in C_n^2, the morning quiescent period. Subsequently C_n^2 rose steadily until just before noon when a passing cloud reduced the solar radiation by 65% for a few minutes causing C_n^2 to drop momentarily by a factor of 8. Around 2:00 PM the conditions became overcast, C_n^2 fell steadily until shortly before sunset when there was a pronounced increase in sunlight that induced an order of magnitude fluctuation in C_n^2. Overnight and throughout the next day, which was sunny and clear, C_n^2 behaved in the usual way with obvious morning and evening transition periods. The third day was marked by heavy cloud cover throughout the day until late in the afternoon. There was no obvious morning transition as C_n^2 fell steadily until the cloud cover broke, about two hours before sunset, at which time it rises quickly peaking just before sunset and the onset of the evening quiescent period. This set of data illustrates that changes in the solar radiation strongly affected C_n^2 for this particular link, a horizontal path approximately 75 meters above ground level.

The deleterious effects of scintillation on the performance of a communication system are best quantified by power-in-fiber measurements at the receiver. In particular, creating a histogram of time series data provides an estimate of the probability distribution function $p(P_f)$. The log-normal distribution[13] failed to yield good agreement with the measured data, especially in instances where the turbulence was strong. The most successful fits were obtained by using the Γ-Γ distribution[10] given by

Downloaded from SPIE Digital Library on 15 Mar 2010 to 18.51.1.125. Terms of Use: http://spiedl.org/terms

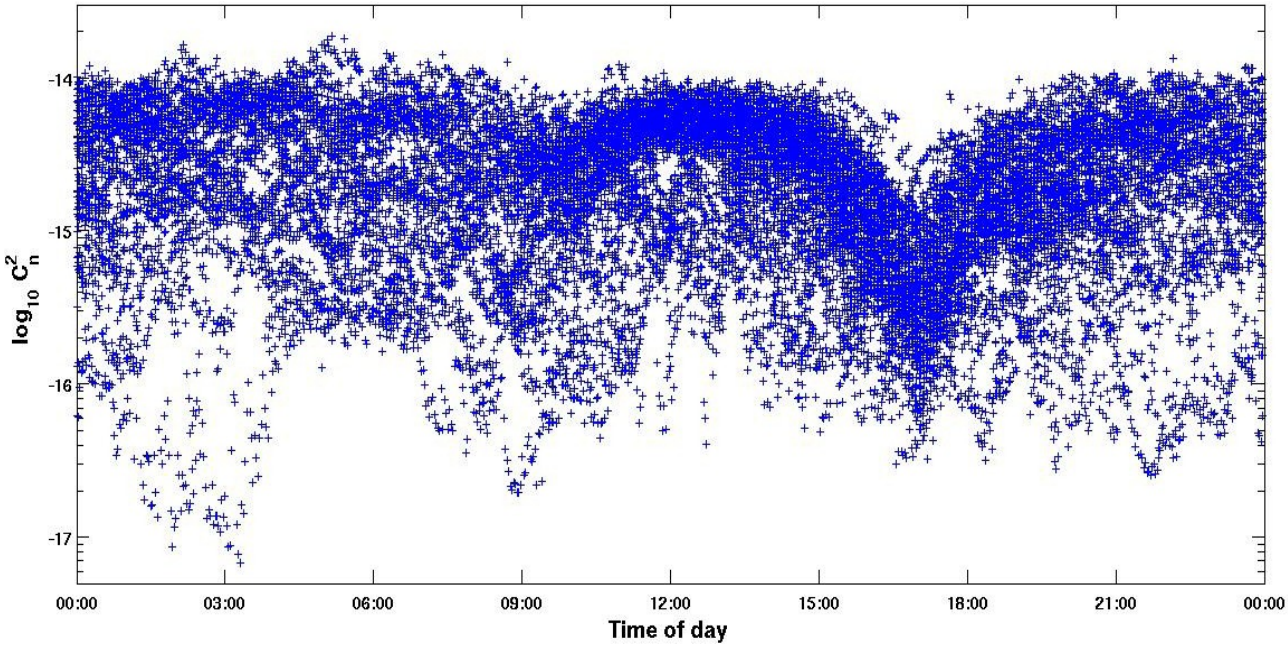

Figure 2. Measured values of C_n^2 for a horizontal 5.4-km link versus time of day for 35 days.

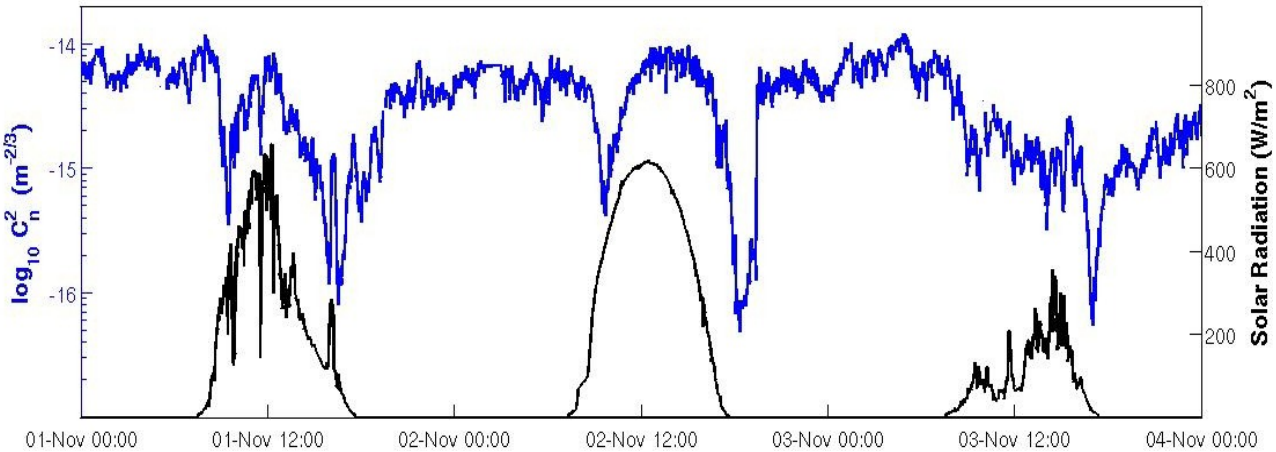

Figure 3. The blue (upper) trace depicts C_n^2 over a period of three days. The black (lower) trace indicates the solar radiation over the same time period.

Downloaded from SPIE Digital Library on 15 Mar 2010 to 18.51.1.125. Terms of Use: http://spiedl.org/terms

Observation Time	C_n^2 $[m^{-2/3}]$	α	β
11:56–11:58	$(0.91 - 1.32) \times 10^{-15}$	26.8	26.8
11:58–12:00	$(1.32 - 2.14) \times 10^{-15}$	18.0	18.0
12:00–12:02	$(2.14 - 4.17) \times 10^{-15}$	10.5	10.5
12:02–12:04	$(4.17 - 5.26) \times 10^{-15}$	5.9	6.1
12:04–12:06	$(5.26 - 6.24) \times 10^{-15}$	5.3	5.3

Table 1. Best fit shape parameters α and β for the five histograms in Fig. 4 and measured values of C_n^2 at the start and finish of the observation period as reported by the scintillometer.

$$p(P_f) = \frac{2(\alpha\beta)^{(\alpha+\beta)/2}}{\Gamma(\alpha)\Gamma(\beta)P_f} \left(\frac{P_f}{<P_f>} \right)^{(\alpha+\beta)/2} K_{\alpha-\beta} \left(2\sqrt{\frac{\alpha\beta P_f}{<P_f>}} \right), P_f > 0, \quad (1)$$

where α and β are shape parameters that are related to C_n^2, $K_r(\cdot)$ is a Bessel function of the second kind of order r and $<P_f>$ is the mean. Determining the probability of fades (i.e., the behavior of the tail) requires an examination of Eq. 1 for values of $P_f \ll <P_f>$ which indicates a power-law dependence.

For the majority of data collected the Γ-Γ distribution provided an excellent fit for the measured fluctuation in $P_f(t)$; however, in some instances the histogram had a tail that did not obey a power-law. Rather, a flared tail indicated the presence of fades that were deeper than predicted by the Γ-Γ model. These flares can be attributed to changes in C_n^2 during the collection of the time series data. In Fig. 4 data for C_n^2, $P_f(t)$, and 5 histograms of $P_f(t)$ illustrate the effect of a quickly changing C_n^2. Over ten minutes C_n^2 increased by nearly an order of magnitude, indicating a shift from benign to moderate turbulence, and the $P_f(t)$ displayed an obvious increase in its variance. When broken up into two-minute intervals the time series data are well described by Γ-Γ distributions; however, when the entire ten-minute period is considered the Γ-Γ distribution fails to describe the tails of the histogram accurately; instead, a better fit is achieved by averaging the fits for the 5 two-minute intervals as is seen in Fig. 5. Table 3 provides the shape parameters as well as the measured values of C_n^2 shown in Fig.4. From the table it is apparent that $\alpha \approx \beta$, while this may not be true for a vertical path through the atmosphere it seems to hold this particular geometry. In a more dramatic example of a departure from the Γ-Γ distribution Fig. 6 shows a histogram constructed from data taken between 3:35 and 4:15, a 40-minute interval, during a partly cloudy day. In this case the histogram has a flared tail which could not be described adequately by a Γ-Γ distribution.

4. DISCUSSION

The strong correlation between C_n^2 and the statistical behavior of $P_f(t)$, which was well described by the Γ-Γ distribution assuming C_n^2 does not vary significantly over the period in question, provides a useful tool for the design of optical communications links propagating through an atmospheric channel. Specific knowledge of the statistical behavior of $P_f(t)$ is essential for the proper implementation of coding and interleaving techniques designed to mitigate errors arising from channel fades. For the duration of the experiment the observed values for C_n^2 varied over more than three orders of magnitude from 8×10^{-18} to $2 \times 10^{-14}\,\mathrm{m}^{-2/3}$ leading to a wide range of fading conditions. Unfortunately, C_n^2 often persisted for hours near the $10^{-14}\,\mathrm{m}^{-2/3}$ level and rarely dropped below $10^{-16}\,\mathrm{m}^{-2/3}$ implying that any high-availability system must consistently combat the strongest turbulence conditions. Moreover, any accurate calculation of the clear line-of-sight link availability must incorporate the variability of C_n^2 into a doubly-stochastic model where the distribution of C_n^2 leads to a distribution of α's and β's from which the long-term distribution of P_f can be determined. It may be feasible to develop adaptive rate systems to take advantage changes in C_n^2; however, those systems must be capable of addressing rapid changes

Downloaded from SPIE Digital Library on 15 Mar 2010 to 18.51.1.125. Terms of Use: http://spiedl.org/terms

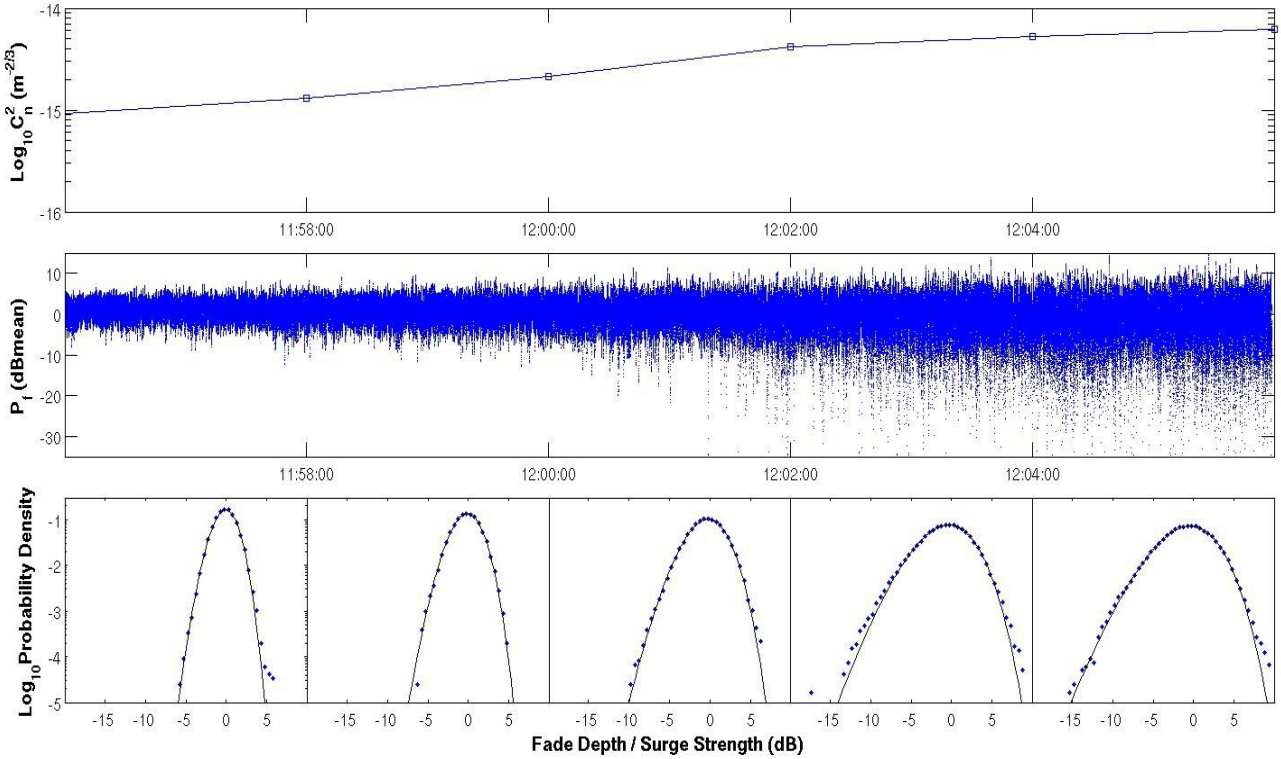

Figure 4. The top graph displays C_n^2over a period of ten minutes. The middle trace is the recorded power in fiber for one of the four receiver chains. Histograms of the power in fiber for two-minutes periods are shown in the five bottom panels along with fits to a Γ-Γdistribution; each panel corresponds to the 2-minute interval directly above it.

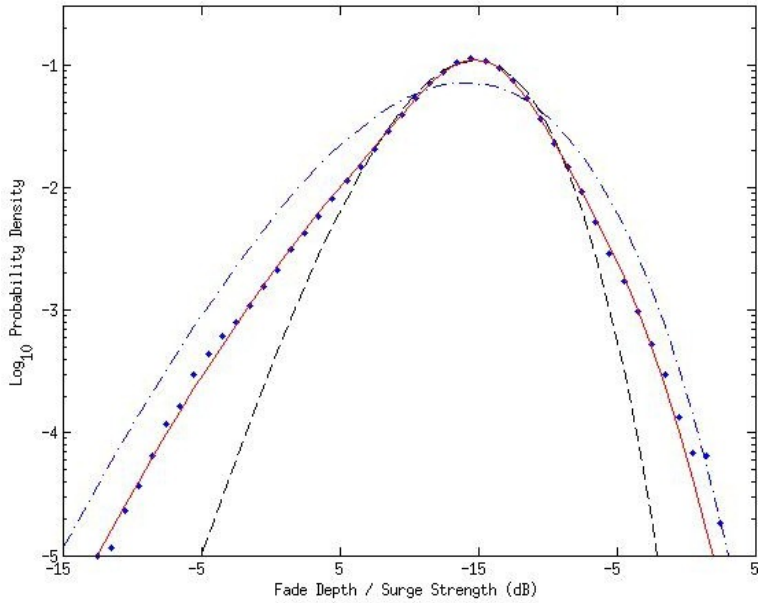

Figure 5. A histogram of the ten-minute time series of $P_f(t)$ shown in Fig. 4. (blue dots). A Γ-Γ fit to the histogram (dashed black curve). The average of fits to each of the 5 two-minute histograms shown in Fig. 4 (red curve). For compariosn the fit to the most turbulent two-minute interval from panel 5 of Fig. 4 (dot-dashed blue curve) is included.

Downloaded from SPIE Digital Library on 15 Mar 2010 to 18.51.1.125. Terms of Use: http://spiedl.org/terms

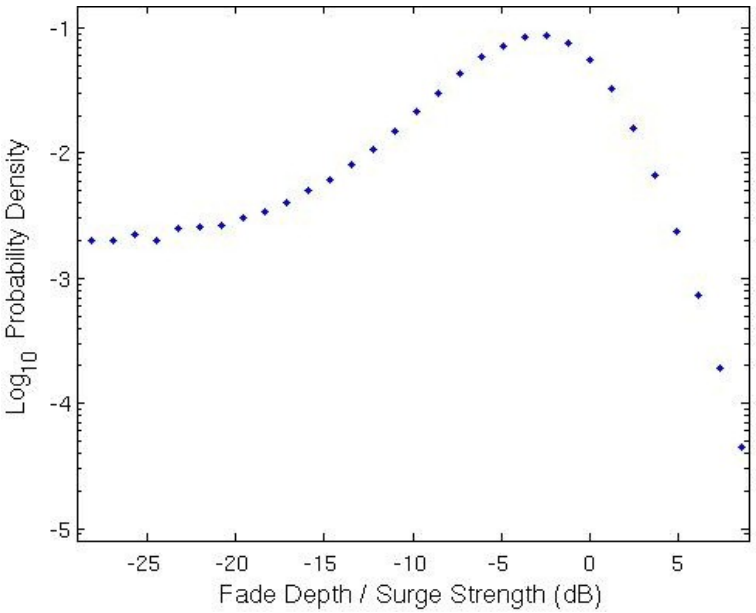

Figure 6. Histogram of the measured P_f taken over a 40-minute period, not overlapping the quiescent period, during which C_n^2 varied from moderate to severe values.

in the value C_n^2 observed in this experiment. Future work may test the models that predict local C_n^2 from environmental inputs,[12] e.g., PAMELA, and use those predictions to set the levels of coding and interleaving to maximize the error-free throughput of the channel.

ACKNOWLEDGMENTS

The authors would like to thank the MIT Westford site staff who supported us, especially Jeff Dominick for hosting our experiment and Jim Hunt for his fearless tower work, the many other staff members of the Advanced Lasercom Systems and Operations group who made this experiment possible, and the Rapid Reaction Technology Office. This work was sponsored by the Department of the Defense under Contract FA8721-05-C-0002. Opinions, interpretations, conclusions, and recommendations are those of the authors and are not necessarily endorsed by the United States Government.

REFERENCES

[1] Lawrence, R. S. and Strohbehn, J. W., "A survey of clear-air propagation effects relevant to optical communications," *IEEE Transactions on Communication* **58** (Oct 1970).

[2] Kim, I. I., Hakakha, H., Adhikari, P., Korevaar, E., and Majumdar, A. K., "Scintillation reduction using multiple transmitters," in [*Proceeding of the SPIE: Free-Space Laser Communication Technologies IX*], **2990**, 102–113 (1997).

[3] Shin, E. J. and Chan, V. W. S., "Optical communication over the turbulent atmospheric channel using spatial diversity," in [*Global Telecommunications Conference*], *GLOBECOM '02* **3** (2002).

[4] Lee, E. J. and Chan, V. W. S., "Part 1: Optical communication over the clear turbulent atmospheric channel using diversity," *IEEE Journal on Selected areas in Communications* **22**, 1896–1906 (Nov. 2004).

[5] Razavi, M. and Shapiro, J. H., "Wireless optical communications via diversity reception and optical preamplification," *IEEE Transactions on wireless Communications* **4**, 975–983 (May 2005).

[6] Proakis, J. G., [*Digital Communications*], McGraw-Hill, New York, NY, fifth ed. (2008).

[7] Cho, P. S., Meiman, Y., Harston, G., Achiam, Y., and Shpantzer, I., "Fading mitigation in homodyne RZ-QPSK via delay-diversity transmission," in [*Coherent Optical Technologies and Applications*], Optical Society of America, paper CWB6 (2008).

Downloaded from SPIE Digital Library on 15 Mar 2010 to 18.51.1.125. Terms of Use: http://spiedl.org/terms

[8] Zhu, X. and Kahn, J., "Free-space optical communication through atmospheric turbulence channels," *IEEE Transactions on Communication* **50** (Aug 2002).
[9] Anguita, J., Djordjevic, I., Neifeld, M., and Vasic, B., "Shannon capacities and error-correction codes for optical atmospheric turbulent channels," *Journal of Optical Networkwing* **4**(9), 586–601 (2005).
[10] Andrews, L. C., Phillips, R. L., and Hopen, C. Y., [*Laser Beam Scintillation with Applications*], SPIE Press, Bellingham, WA (2001).
[11] Sasiela, R. J., [*Electromagnetic Wave Propagation in Turbulence*], SPIE Press, Bellingham, WA (2007).
[12] Majumdar, A. K. and Ricklin, J. C., [*Free-Space Laser Communications*], Springer, New York, NY (2008).
[13] Andrews, L. C., [*Field Guide to Atmospheric Optics*], SPIE Press, Bellingham, WA (2004).

Downloaded from SPIE Digital Library on 15 Mar 2010 to 18.51.1.125. Terms of Use: http://spiedl.org/terms